

# Design and Analysis of Rectangular Spiral Nano-Antenna for Solar Energy Harvesting

Fatma M. Abdel Hamied<sup>1, \*</sup>, Korany R. Mahmoud<sup>1, 2</sup>,  
Mohamed Hussein<sup>3, 4, 5</sup>, and Salah S. A. Obayya<sup>3</sup>

**Abstract**—Recently, optical nano-antennas (NAs) have been introduced as an alternative approach for photovoltaics devices in solar power harvesting application. In this work, we introduce a new modification to the conventional Archimedean spiral NA to improve its radiation/harvesting efficiency and directivity. The proposed design is a rectangular spiral NA of two tip-to-tip opposing arms which are separated by an air gap. The reported design performance is investigated in terms of the radiation efficiency, directivity, polarization, radiation pattern, and total harvesting efficiency. The numerical study is carried out using the finite integration technique (FIT) within the wavelength range 300–1600 nm. The presented design offers a maximum radiation efficiency of 88% without substrate and 97.9% on top of the silicon dioxide (SiO<sub>2</sub>) substrate at a wavelength of 500 nm where the maximum radiation of the sun occurs. In addition, the proposed design has a maximum directivity of 10.8 without substrate which is increased to 19.1 on top of a substrate at 500 nm. It is found that the suggested rectangular design shows an enhancement in the radiation efficiency and directivity over the counterpart Archimedean nano-spiral antenna by 10% and 208%, respectively. The proposed rectangular design introduces total harvesting efficiencies of 96.2% and 98.1% without and with substrate, respectively. Moreover, the effect of round edges that may appear in the fabrication process is also considered.

## 1. INTRODUCTION

During the last years, an extraordinary increase in the worldwide energy demand has been witnessed as a consequence of growing world population and depleting fossil fuel. This deserves searching for alternative clean and renewable energy sources. Solar power is considered as one of the renewable energy sources and is widely used due to its availability. Several techniques have been used for collecting the solar energy. The photovoltaic (PV) technology is considered the most commonly used one [1]. The conventional PV solar cell collects solar radiation only from the visible region (0.4–0.7  $\mu\text{m}$ ) and converts it into electricity [2, 3]. However, solar cells have several disadvantages such as low conversion efficiency ( $\sim 30\%$ ), requiring a mechanical sun-tracking system to normal incidence of solar irradiance, and their efficiencies are limited by semiconductor band gap energy. To exploit the IR (0.7–100  $\mu\text{m}$ ) region and overcome the previous disadvantages, nano-rectenna is considered as an alternative approach to PV technology [1, 4, 5]. Nano-rectenna converts the incoming electromagnetic radiation into DC electricity. Nano-rectenna stands for a rectifying-antenna [6], and it is a combination of submicron antenna and built in ultra-high speed rectifier diode [7]. When the radiation is incident on NA, an AC signal will be stimulated on the NA arms, and hence an electric field will be accumulated at the antenna feed

---

*Received 12 January 2021, Accepted 6 March 2021, Scheduled 13 March 2021*

\* Corresponding author: Fatma Moawad Abdel Hamied (engfatmamoawad@gmail.com).

<sup>1</sup> Electronics, Communications, and Computers Department, Faculty of Engineering, Helwan University, Cairo, Egypt. <sup>2</sup> National Telecommunications Regulatory Authority, Ministry of Communication and Information Technology, Giza, Egypt. <sup>3</sup> Centre for Photonics and Smart Materials, Zewail City of Science and Technology, October Gardens, 6th of October City, Giza 12578, Egypt.

<sup>4</sup> Department of Physics, Faculty of Science, Ain Shams University, Abbassia, Cairo 11566, Egypt. <sup>5</sup> Light Technology Institute, Karlsruhe Institute of Technology, Engesserstrasse 13, Karlsruhe 76131, Germany.

point [8], where the diode is connected to rectify the received power into DC power [9]. Nano-rectenna theoretical harvesting efficiency is high ( $\sim 100\%$ ) [10] as compared to PV solar cells.

In this context, Vandenbosch and Ma [11] derive upper limits for solar energy harvesting efficiency using NAs. They studied the effect of NA dimensions and NA materials (Al, Au, Cr, Cu, and Ag) and on the harvesting efficiency. From the simulation results, silver showed the highest efficiency of  $\sim 90\%$  in both free space and on the substrate. Moreover, Yan et al. [12] designed a bowtie nano-rectenna for solar energy harvesting applications on top of a silicon dioxide ( $\text{SiO}_2$ ) substrate with the total radiation efficiency of 61%. Additionally, Hussein et al. [13] designed a flower-shaped dipole NA to enhance the radiation efficiency, within wavelength range from 400 to 1400 nm. The proposed design [13] has achieved a high harvesting efficiency of 74.6% at 500 nm. Further, El-Toukhy et al. [14] designed a tapered dipole antenna with a total harvesting efficiency of 79.2%. Sallam et al. [15] introduced a design of wire-grid NA array with circularly polarized radiation on a silicon dioxide ( $\text{SiO}_2$ ) substrate backed by a thick layer of silver for wireless optical communication systems with a radiation efficiency of 82.75% at 193.55 THz and directivity of 10.8 dBi. Zhao et al. [16] designed an Archimedean nanospiral antenna for solar energy application with a high harvesting efficiency of about 80% at a wavelength of 500 nm and a maximum directivity about 3.5. In 2020, Elsaïd et al. [17] proposed and analyzed an optimized four-nanowire rhombic NA in terms of directivity and efficiency. Elsaïd's design achieved a directivity of 23.4 and radiation efficiency of 84.5% at a wavelength of 1550 nm. Also, in 2020, Ranga et al. [18] designed a NA of a petal shape, and the effect of changing the NA geometrical parameters (height, width, length and gap) on radiation/harvesting efficiency was studied. Various types of NA material have also been studied.

In this paper, the 3D finite integration technique (FIT) [17] is utilized to investigate and analyze the performance of the suggested rectangular spiral NA. A spiral NA is particularly chosen in our work as it is efficient in collecting the solar energy, and it is a frequency independent NA which operates over a wide frequency range. It has high electric field enhancement, and it can receive from any polarized light because of its circular polarization. The nano-spiral can be easily connected to a high resistance diode. The optical characterization of the presented NA is studied in terms of the directivity, radiation efficiency, and radiation pattern. The objective of this design is to obtain a higher efficiency than that reported in [16] at the wavelength of 500 nm where the maximum radiation of the sun occurs. In this regard, the proposed design with sharp edges has a maximum radiation efficiency of 88% in free space and 97.9% on a substrate of silicon dioxide ( $\text{SiO}_2$ ) at 500 nm. Furthermore, the radiation efficiency and directivity have been enhanced by 10% and 208%, respectively, over the Archimedean spiral NA reported in [16].

The present paper is organized as follows. A brief explanation of the NA parameters is introduced in Section 2. A description of the NA topology and simulation methodology are illustrated in Section 3. In Section 4, detailed numerical results are presented. Finally, conclusions will be discussed in Section 5.

## 2. NANO-RECTENNA PERFORMANCE PARAMETER

The nano-rectennas performance depends on the efficiency by which the light is collected and converted into AC power at NA terminals and the matching between the diode and NA impedances, as well as the efficiency by which the harvested light is converted to DC power by the diode (rectifier). Undoubtedly, the antenna directivity,  $D$ , plays an important role regarding the performance. The NA directivity is a measure of the capability of the NA to concentrate the radiated power in a certain direction, which can be expressed as follows [19]:

$$D = \frac{4\pi}{P_r} P(\theta, \emptyset) \quad (\text{dimensionless}) \quad (1)$$

where  $\theta$  is the azimuthal angle,  $\emptyset$  the elevation angle,  $P_r$  the radiated power from the NA, and  $P(\theta, \emptyset)$  the angular power density. Due to the reciprocity theory [2, 20, 21], the efficiency of NA at reception (harvesting efficiency) is the same as that at the transmission, which is known as the radiation efficiency  $\eta^r$  of the NA [22]. The NA radiation efficiency is a key parameter in the total harvesting efficiency by which the NA can convert the incident electromagnetic radiation into useful energy. The NA radiation efficiency is the ratio of the radiated power from the NA to the total injected power at the NA input

port,  $P_i$ , which can be evaluated as follows:

$$\eta^r = \frac{P_r}{P_i} = \frac{P_r}{P_r + P_L} \quad (2)$$

where  $P_L$  is the total loss power (the power actually dissipated in the NA material). For solar energy harvesting application, the total harvesting efficiency of the nano-rectenna is the ratio of output DC power rectified through the diode ( $P_{rec}$ ) to the optical input power ( $P_{opt}$ ), which can be calculated as follows:

$$\eta^{tot} = \frac{P_{rec}}{P_{opt}} \quad (3)$$

With some analysis reported in details in [22], the closed formula for the total harvesting efficiency of the optical nano-rectenna is as follows:

$$\eta^{tot} = \frac{\int_0^\infty P(\lambda, T) \eta^r(\lambda) d\lambda}{\int_0^\infty P(\lambda, T) d\lambda} \quad (4)$$

where  $\lambda$  is the wavelength of the incident light, and  $P$  is the Planck's formula for black body radiation (incident power density) given by:

$$P(\lambda, T) = \frac{2\pi hc^2}{\lambda^5} \frac{1}{(\exp(hc/\lambda KT) - 1)} \quad (5)$$

Also,  $T$  is the blackbody absolute temperature (in °K); while in the case of solar power applications,  $T$  is the sun surface temperature.  $h$  is Planck's constant ( $6.626 \times 10^{-34}$  Js),  $K$  the Boltzmann constant ( $1.38 \times 10^{-23}$  J/K), and  $C$  the light speed in vacuum ( $3 \times 10^8$  m/s).

This efficiency ( $\eta^{tot}$ ) takes into account the effect of the losses in the NA but does not take the effect of the mismatch losses (assume perfect matching between the NA and diode impedances).

As described above, nano-rectenna consists of a receiving NA and a rectifying diode that rectifies the received signal into DC electricity. The equivalent circuit of the NA integrated with MIM diode is shown in Fig. 1. The NA in a receiving mode is represented by impedance,  $Z_A = R_A + jX_A$ , in series with an AC voltage source,  $V_{AC}$ . The MIM tunnel diode can be represented as a parallel combination of capacitor,  $C_D$ , and nonlinear resistance,  $R_D$ .

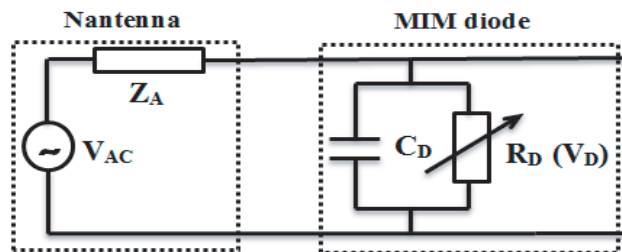


**Figure 1.** The equivalent circuit of nano-antenna (NA) coupled to MIM diode [23].

The received power by the diode rectifier is given by [23]:

$$P_{rec} = \frac{1}{2} (V_{AC})^2 \frac{R_D}{|Z_A + Z_D|^2} \quad (6)$$

where  $Z_{rec} = R_{rec} + jX_{rec}$  is the rectifier impedance.  $V_{AC}$  can be expressed in terms of the incident electric field,  $E_{inc}$ , and the effective area  $A_{ef}$ .

$$V_{AC} = 2\sqrt{\frac{R_A A_{ef}}{Z_0}} E_{inc} \quad (7)$$

whereas the effective area can be expressed in terms of the antenna gain,  $G$ , with classical formula

$$A_{ef} = \frac{\lambda^2 G}{4\pi} \quad (8)$$

The incident electric field amplitude can be expressed in terms of the incident power density as:

$$|E_{inc}| = \sqrt{2Z_0 P(\lambda, T)} \quad (9)$$

Then, the output power of nano-rectenna will be expressed as:

$$P_{rec} = A_{ef}^{\max} \eta^{\text{mat}} P(\lambda, T) \eta^r \quad (10)$$

where  $\eta^{\text{mat}}$  is the matching efficiency which mainly depends on the NA and rectifier impedances. Due to the dependency of the impedances and gain on the wavelength, an integration has to be performed over the investigated wavelength band. Therefore, the final formula for the output power of nano-rectenna will be:

$$P_{rec} = \int_{\lambda_{start}}^{\lambda_{end}} A_{ef}^{\max}(\lambda) \eta^{\text{mat}}(\lambda) P(\lambda, T) \eta^r(\lambda) d\lambda \quad (11)$$

where  $\lambda_{start}$  and  $\lambda_{end}$  are the starting and ending wavelengths of the investigated band, and  $Z_o$  is the free space intrinsic impedance ( $377 \Omega$ ). In case of perfect matching between the rectifier and the NA impedances,  $\eta^{\text{mat}}$  will equal 1 (i.e.,  $\eta^{\text{mat}} = 1$ ).

### 3. NA TOPOLOGY AND SIMULATION METHODOLOGY

Since our work concentrates on the effect of various antenna designs on solar energy harvesting, the proposed NA is considered in free space (without substrate) and on top of a substrate. The objective of the proposed design is to improve the radiation/harvesting efficiency and directivity of the Archimedean spiral NA [16] at 500 nm. The Archimedean spiral NA consists of two silver arms separated by gap distance of 10 nm. The geometrical parameters of the Archimedean spiral NA are  $G = 40$  nm, width  $W = 40$  nm, and thickness 40 nm as shown in Fig. 2(a). The proposed design is a rectangular spiral NA which consists of two arms facing each other tip-to-tip and separated by a gap distance  $g = 10$  nm, as shown in Fig. 2(b). Each arm has 1.5 turns and is made of silver, due to the high conductivity of the silver. To optimize the rectenna design, a parametric sweep (tuning process) method for different parameters is applied to study the effect of changing the geometrical parameters on the radiation efficiency and directivity of the proposed design. The rectangular spiral NA geometrical parameters in  $X$ - $Y$  plane are  $L_1 = 100$  nm,  $L_2 = 140$  nm, spacing between the two arms  $G = 40$  nm and width  $W = 40$  nm. The proposed design has a fixed thickness of 60 nm at  $Z$ -axis, excited by a plane wave

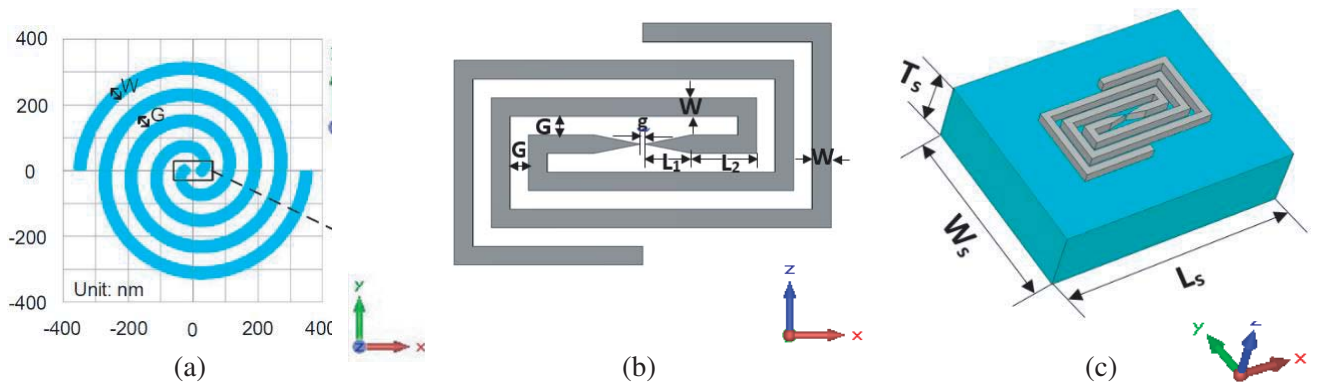


**Figure 2.** The NA designs. (a) Archimedean design [16]. (b) Proposed NA top view without substrate. (c) 3D view of the proposed design with glass substrate ( $\text{SiO}_2$ ).

normal to  $Z$ -axis, and circular polarization parallel to  $X$ -axis with an electric field intensity of  $1 \text{ V/m}$ . The constructed model uses a minimum mesh size of  $4.5 \text{ nm}$  and is surrounded by free space everywhere. The spiral NA is picked out in our work as it is efficient in collecting the solar energy, and it has high electric field concentration in the antenna gap. Generally, sunlight is randomly polarized, and consequently, circularly polarized antennas can harvest the light efficiently at different polarizations. Therefore, antenna radiation characteristics of the proposed spiral NA such as polarization, radiation pattern, and impedance are stable over large bandwidth. Actually, in the fabrication process, NAs must be placed on a substrate, which has a great effect on the radiation characteristics of the NA as a result of the plasmonic effects [24], hence substrate is investigated in our study. The substrate must be much thicker than the wavelength, to be of major effect. The effect of a substrate is studied, in terms of various materials, different thickness, length, and width. The substrate is composed of silicon dioxide ( $\text{SiO}_2$ ) material, has length  $L_s$  of  $1370 \text{ nm}$ , width  $W_s$  of  $1080 \text{ nm}$ , and thickness  $T_s$  of  $400 \text{ nm}$ , and shows the highest radiation efficiency and directivity at  $500 \text{ nm}$ . Fig. 2(c) shows three dimensional view of the suggested NA with glass substrate ( $\text{SiO}_2$ ). The finite integration technique (FIT) is employed in this study, where the NAs radiation efficiency, directivity, and radiation pattern are calculated at  $\lambda = 500 \text{ nm}$ . The main advantages of the FIT [25–27] are backed to its high flexibility in modeling complex geometries, both in time and frequency domains.

To check the validity of the numerical results, the conventional dipole NA (CDNA) reported by Vandenbosch and Ma [11] was first simulated and analyzed. The schematic diagram of the CDNA is inserted in Fig. 3. The studied CDNA consists of two arms of rectangular shape, and each of them has length  $L$  of  $250 \text{ nm}$ , width  $W$  of  $40 \text{ nm}$ , and thickness  $T$  of  $40 \text{ nm}$ . The two arms are separated by a gap  $g = 10 \text{ nm}$ . Fig. 3 shows the radiation efficiency versus the wavelength calculated using FIT technique and compared to that calculated by MOM method reported in [11]. It can be seen from this figure that a good agreement is obtained between our results by FIT and previously reported in [11], and the small deviation between the two curves can be attributed to two reasons. First, the constructed model in our study is based on finite integration technique which is a well-known method for its accuracy and high precision. Additionally, the reference calculations, reported in [11], are based on a finite difference time domain (FDTD) technique. Therefore, the variation in the numerical results shown in the following figure can be attributed to different techniques used in calculations.

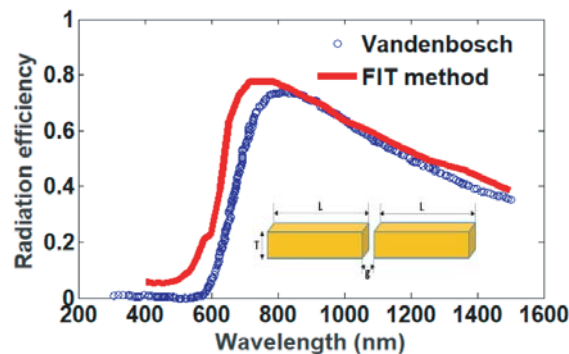


**Figure 3.** The radiation efficiency variation with the wavelength for the CDNA, calculated using FIT method and compared to that reported by Vandenbosch et al. calculated by MOM technique [11].

#### 4. NUMERICAL RESULTS

Since NA must be manufactured on a supporting layer, the influence of the substrate is investigated. By using higher dielectric constant ( $\epsilon_r$ ) of the substrate material, the spiral NA performance decreases [28], so the silicon dioxide material ( $\text{SiO}_2$ ) is chosen as a substrate layer due to its smaller permittivity. For the considered frequency range, the permittivity of  $\text{SiO}_2$  is almost constant and about 2.39.

Figures 4(a) and 4(b) illustrate the 3D radiation patterns for the proposed spiral NAs without and with substrate, respectively, at  $\lambda = 500 \text{ nm}$ . It is found that the proposed design without substrate

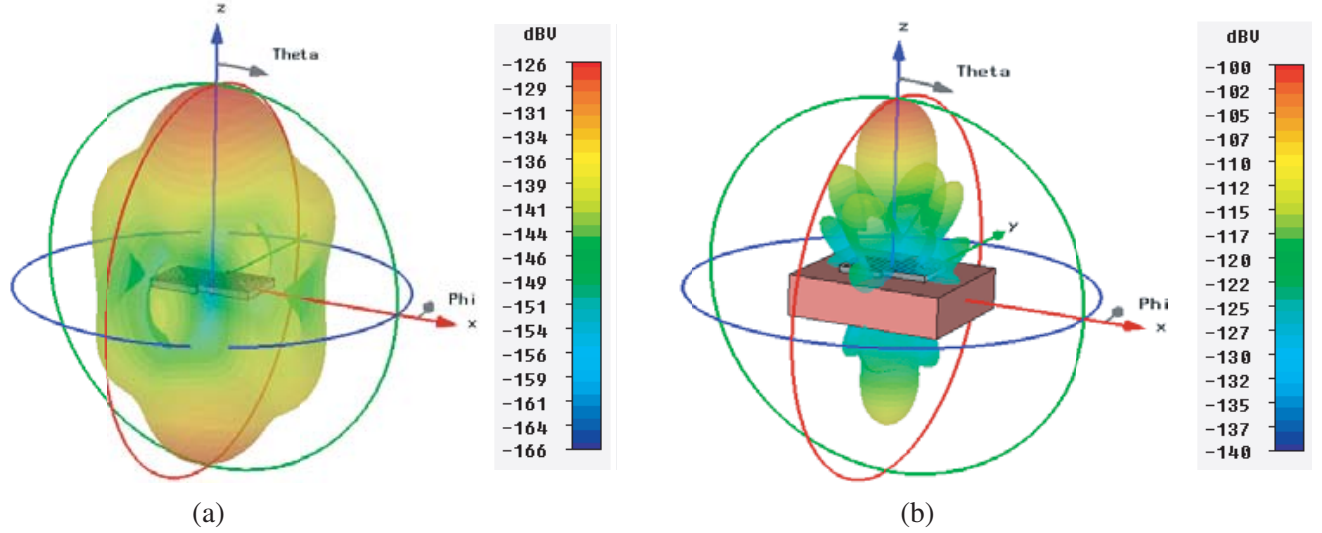


**Figure 4.** Three-dimensional E-patterns at 500 nm for (a) the proposed spiral NA in free space (without substrate), (b) the proposed spiral NA with a substrate.

can provide an angular beamwidth of  $46.5^\circ$ , which is decreased to  $21.2^\circ$  using substrate. On the other hand, the design with a substrate decreases the side lobe level from  $-9.6$  dB to  $-2$  dB, in addition to increasing the NA directivity and efficiency by 76.85% and 11.25%, respectively, at 500 nm.

Figure 5(a) shows the radiation efficiency versus the wavelength for the proposed rectangular spiral NA in free space, with substrate and that of the convolutional Archimedean spiral NA [16], respectively. The proposed NA achieves a maximum  $\eta^r$  of 88% at  $\lambda = 500$  nm with high total harvesting efficiency of 96.2% (assuming ideal rectifier) and total received power of  $1.6121 \times 10^{-13}$  W, without substrate. These results improve radiation efficiency of the Archimedean nanospiral antenna [16] by 10% and the total harvesting efficiency by 15.9%. Moreover, the designed NA effectively acts as an ultra-wideband antenna within the wavelength range 600–1600 nm, whereas the radiation efficiency roughly remains constant. Fig. 5(b) shows the directivity for the proposed NA in free space, on top of the substrate, and that of the Archimedean nanospiral antenna, respectively. The directivity has a maximum value at 300 nm and decreases with increasing the wavelength due to the spiral NA truncation. It is also obvious that the proposed NA offers a maximum directivity of 10.8 at 500 nm in free space, which is larger than that of Archimedean nanospiral by 208%. It is a distinguished result as a larger directivity corresponds to a greater effective area according to Eq. (5), which means that more solar power will

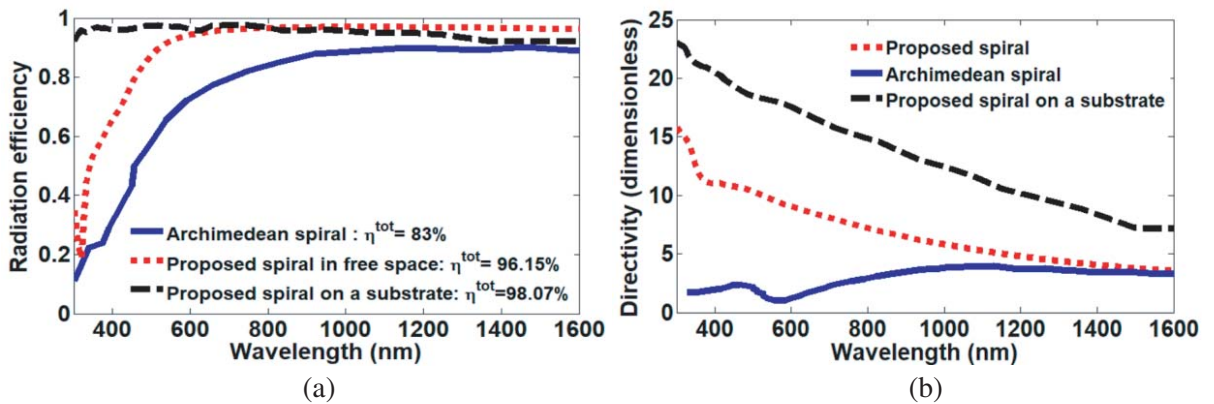


**Figure 5.** The radiation characteristics of Archimedean spiral antenna, the proposed NA in a free space and with substrate versus wavelength. (a) The radiation efficiency. (b) The directivity.

be collected. Therefore, a larger directivity as well as higher radiation efficiency for the nanospiral will lead to a larger effective area, which permits more power received by the NA to be rectified without dissipating it by the antenna material.

On the other hand, the suggested NA on top of a substrate achieves a maximum radiation efficiency of 97.9% at the wavelength of 500 nm with the total harvesting efficiency of 98.1% (assuming ideal rectifier) and total received power of  $3.3639 \times 10^{-13}$  W as shown in Fig. 5(a). It is obvious that the substrate makes a great effect because of its high thickness and low dielectric constant of material. The obtained efficiency in the case of substrate is larger than that in free space. Furthermore, the proposed NA on a substrate can achieve a maximum directivity of 19.1 at 500 nm as shown in Fig. 5(b). Therefore, the suggested NA with a substrate has a great enhancement in the antenna characteristics.

By launching a normally incident plane wave with linear polarization parallel to  $X$ -axis and electric field intensity of 1 V/m, the absolute value of the electric field intensity can be calculated at the NA gap. Fig. 6 demonstrates the wavelength dependent field intensity at the NA gap for the proposed rectangular spiral NA in free space and on the substrate. Moreover, the obtained values of the electric field intensity at the gap were 6.2 for the reported design in free space and 18.9 for the reported design with substrate at 500 nm.

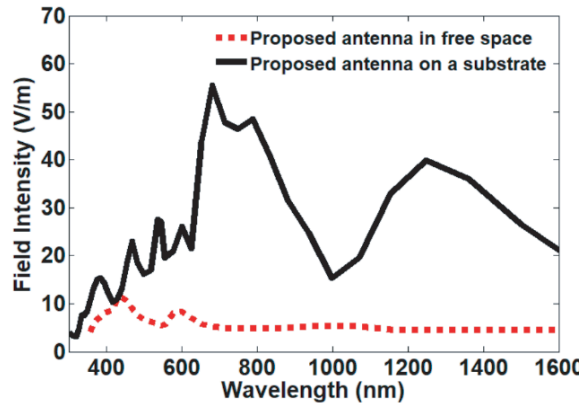


**Figure 6.** Wavelength dependent field intensity at the antenna gap for the proposed rectangular spiral NA in free space and on the glass substrate.

The polarization of a NA is a distinguished feature that affects its application in solar energy harvesting. NAs with different polarizations will absorb different amounts of power when being irradiated by optical signal due to the random polarization of the solar radiation. Therefore, the field intensity is calculated by varying the polarization direction of incident plane wave at 500 nm to study the effect of polarization. Fig. 7 shows the electric field distribution in  $xy$  plane for the proposed rectangular spiral NA at different polarization angles  $\theta = 0^\circ$ ,  $45^\circ$ , and  $90^\circ$  at the wavelength of 500 nm.

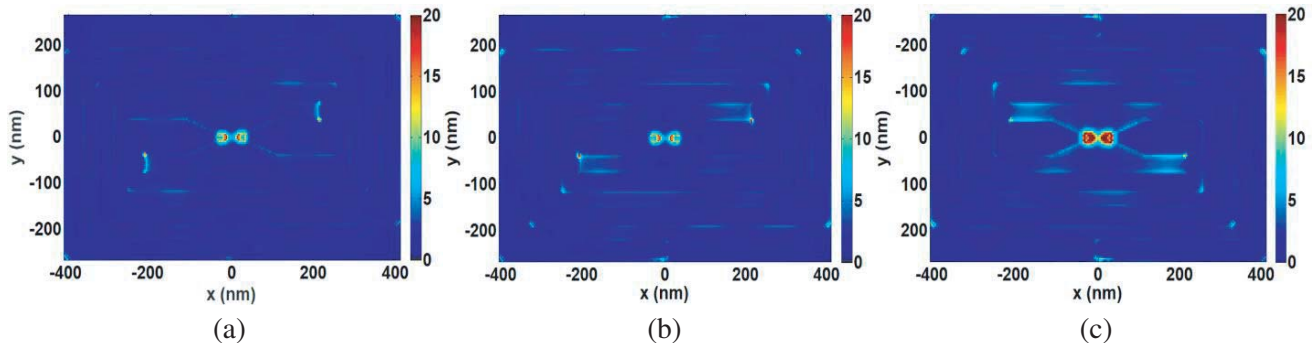


**Figure 7.** The electric field distribution for the proposed rectangular spiral NA at the wavelength of 500 nm in  $x$ - $y$  plane for polarization angles. (a)  $\theta = 0^\circ$ , (b)  $\theta = 45^\circ$  and (c)  $\theta = 90^\circ$ .

It is clear that the electric field is more concentrated in the hot spot (gap area) at polarization angles  $\theta = 90^\circ$ . A significant electric field enhancement occurs at the NA gap, which is mainly attributed to the sharp tips at NA gap. Therefore, the phase and group velocities of the surface plasmon waves tend to go to zero at the tips, leading to exceedingly localized fields and higher harvesting efficiency. On the other hand, a weak electric field is observed on the antenna surface. The proposed nano-spiral can offer a stronger field improvement in the gap, which consequently increases the voltage across the rectifier.

Actually, in the fabrication process, the tapering edges are rounded, so the effect of round edges is investigated to consider the imperfections that may occur in the fabrication process. The geometrical parameters of proposed NA of circular corners are the same as that of the spiral antenna shown in Fig. 2, but the corners are curved with a radius  $R$  as shown in Fig. 8(a). Fig. 8(b) shows three-dimensional view of the NA of round edges on top of a glass substrate ( $\text{SiO}_2$ ). The impact of the radius change is studied, but it is found that the radiation efficiency and directivity are less sensitive to the radius change, as in Fig. 9.

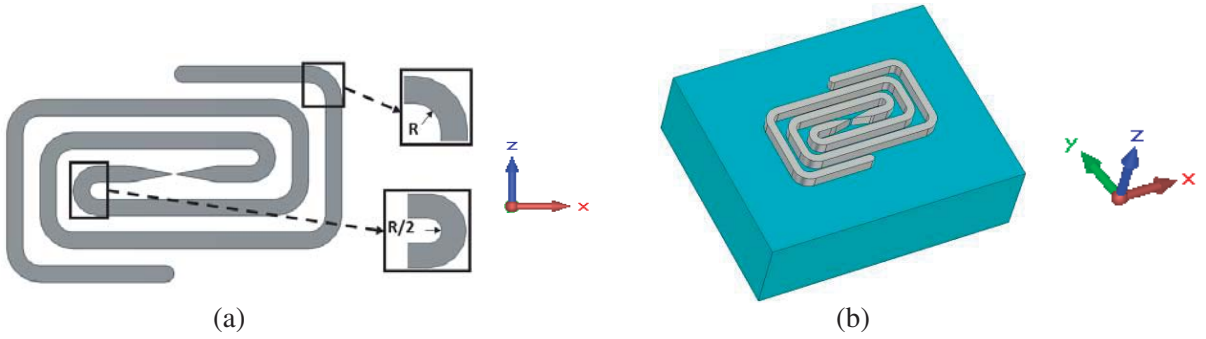


**Figure 8.** The proposed spiral NA of round edges. (a) Top view of the proposed NA of round edges in free space (without substrate). (b) Three dimensional view of the NA of round edges on top of a glass substrate ( $\text{SiO}_2$ ).

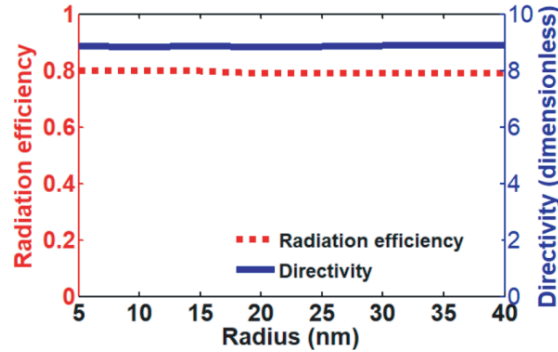


**Figure 9.** The variation of radiation efficiency and the directivity of the proposed rectangular spiral NA of rounded edges with the radius.

Figure 10(a) shows the radiation efficiency versus the wavelength for the proposed round edged rectangular spiral NA of a radius  $R = 40$  nm in free space and with  $\text{SiO}_2$  substrate, respectively. It is found that the proposed rectangular spiral NA of round edges achieves a maximum radiation efficiency of 80% in a free space and 96.8% when being put on the substrate at 500 nm. Moreover, the suggested design of round edges also presents total harvesting efficiencies of 77.8% and 97.7% in free space and on the substrate, respectively. Fig. 10(b) demonstrates the directivity for this NA in free space and on top of the substrate, respectively. This proposed NA offers a maximum directivity of 8.9 in free space and increases to 19.1 on top of the substrate at 500 nm.

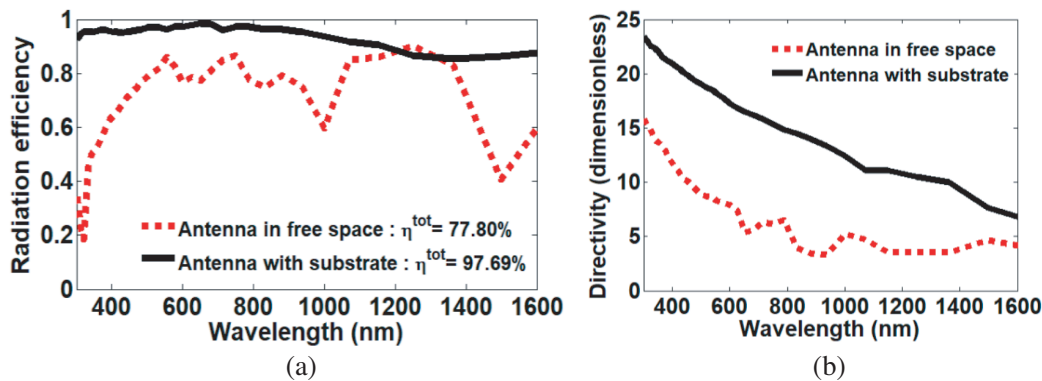


**Figure 10.** (a) The radiation efficiency of the proposed NA of round edges in a free space and on top of a substrate. (b) The directivity of the proposed NA of round edges in free space and on top of a substrate.

## 5. CONCLUSIONS

In this work, a new spiral NA of rectangular shape for solar energy harvesting was investigated and analyzed using the finite integration technique (FIT). The suggested rectangular spiral NA with sharp edges shows a higher radiation efficiency over Archimedean spiral nano-antenna by 10%. In addition, the directivity is improved by 208%. Moreover, the proposed NA of sharp edges offers a broadband in the wavelength range from 300 to 1600 nm and has a high radiation efficiency of 88% in free space at  $\lambda = 500$  nm with the total harvesting efficiency of 96.2%. Moreover, this proposed spiral nano-antenna on the substrate offers a maximum radiation efficiency of 97.9% at 500 nm and total harvesting efficiency of 98.1%. It is expected that results of the spiral nano-antenna will drive us to harvest renewable and clean energy from the environment with higher efficiencies and within a wide bandwidth.

## ACKNOWLEDGMENT

The authors would like to express their gratitude to the National Telecommunication Regulatory Authority (NTRA), Ministry of Communication and Information Technology in Egypt for their support.

## REFERENCES

1. Joshi, S. and G. Moddel, "Rectennas at optical frequencies: How to analyze the response?," *Journal of Applied Physics*, Vol. 118, No. 8, 084503, 2015.
2. Bagher, A. M., M. M. A. Vahid, and M. Mohsen, "Types of solar cells and application," *American Journal of Optics and Photonics*, Vol. 3, No. 5, 94–113, 2015.
3. Eldin, A. H., M. Refaey, and A. Farghly, "A review on photovoltaic solar energy technology and its efficiency," *17th International Middle-East Power System Conference (MEPCON'15), at Mansoura University, Egypt*, 1–7, 2015.
4. Sabaawi, A. M., C. C. Tsimenidis, and B. S. Sharif, "Analysis and modeling of infrared solar rectennas," *IEEE Journal of Selected Topics in Quantum Electronics*, Vol. 19, No. 3, 9000208–9000208, 2013.
5. Moddel, G. and S. Grover, *Rectenna Solar Cells*, Springer, 2013.
6. Mescia, L. and A. Massaro, "New trends in energy harvesting from earth long-wave infrared emission," *Advances in Materials Science and Engineering*, Vol. 2014, 2014.
7. Grover, S. and G. Moddel, "Applicability of Metal/Insulator/Metal (MIM) diodes to solar rectennas," *IEEE Journal of Photovoltaics*, Vol. 1, No. 1, 78–83, 2011.

8. Di Garbo, C., P. Livreri, and G. Vitale, "Review of infrared nanoantennas for energy harvesting," *International Conference on Modern Electrical Power Engineering (ICMEPE-2016)*, 2016.
9. Zhu, Z., S. Joshi, and G. Moddel, "High performance room temperature rectenna IR detectors using graphene geometric diodes," *IEEE Journal of Selected Topics in Quantum Electronics*, Vol. 20, No. 6, 70–78, 2014.
10. Gadalla, M. N., M. Abdel-Rahman, and A. Shamim, "Design, optimization and fabrication of a 28.3 THz nano-rectenna for infrared detection and rectification," *Scientific reports*, Vol. 4, 4270, 2014.
11. Vandenbosch, G. A. and Z. Ma, "Upper bounds for the solar energy harvesting efficiency of nano-antennas," *Nano Energy*, Vol. 1, No. 3, 494–502, 2012.
12. Yan, S., B. Tumendemberel, X. Zheng, V. Volskiy, G. A. Vandenbosch, and V. V. Moshchalkov, "Optimizing the bowtie nano-rectenna topology for solar energy harvesting applications," *Solar Energy*, Vol. 157, 259–262, 2017.
13. Hussein, M., N. F. F. Areed, M. F. O. Hameed, and S. S. A. Obayya, "Design of flower-shaped dipole nano-antenna for energy harvesting," *IET Optoelectronics*, Vol. 8, No. 4, 167–173, 2014.
14. El-Toukhy, Y. M., M. Hussein, M. F. O. Hameed, A. Heikal, M. Abd-Elrazzak, and S. Obayya, "Optimized tapered dipole nanoantenna as efficient energy harvester," *Optics Express*, Vol. 24, No. 14, A1107–A1122, 2016.
15. Sallam, M. O., G. A. Vandenbosch, G. G. Gielen, and E. A. Soliman, "Novel wire-grid nano-antenna array with circularly polarized radiation for wireless optical communication systems," *Journal of Lightwave Technology*, Vol. 35, No. 21, 4700–4706, 2017.
16. Zhao, H., H. Gao, T. Cao, and B. Li, "Efficient full-spectrum utilization, reception and conversion of solar energy by broad-band nanospiral antenna," *Optics Express*, Vol. 26, No. 2, A178–A191, 2018.
17. Elsaid, M., K. R. Mahmoud, M. F. O. Hameed, S. Obayya, and M. Hussein, "Broadband directional rhombic nanoantenna for optical wireless communications systems," *JOSA B*, Vol. 37, No. 4, 1183–1189, 2020.
18. Ranga, R., Y. Kalra, and K. Kishor, "Petal shaped nanoantenna for solar energy harvesting," *Journal of Optics*, Vol. 22, No. 3, 035001, 2020.
19. Balanis, C. A., *Antenna Theory: Analysis and Design*, John Wiley & Sons, 2016.
20. Kotter, D. K., S. D. Novack, W. Slafer, and P. Pinhero, "Theory and manufacturing processes of solar nanoantenna electromagnetic collectors," *Journal of Solar Energy Engineering*, Vol. 132, No. 1, 011014, 2010.
21. Wei, C., S. P. Lewis, E. Mele, and A. M. Rappe, "Reciprocity theorems and pseudoelectric fields for ab initio force calculations," *Physical Review B*, Vol. 55, No. 23, 15356, 1997.
22. Stutzman W. L., and G. A. Thiele, *Antenna Theory and Design*, John Wiley & Sons, 2012.
23. Obayya, S., N. F. F. Areed, M. F. O. Hameed, and M. H. Abdelrazik, "Optical nano-antennas for energy harvesting," *Innovative Materials and Systems for Energy Harvesting Applications*, 26–62, IGI Global, 2015.
24. Soliman, E. A., M. O. Sallam, and G. A. Vandenbosch, "Plasmonic grid array of gold nanorods for point-to-point optical communications," *Journal of Lightwave Technology*, Vol. 32, No. 24, 4898–4904, 2014.
25. Costa, J. R. and J. Guterman, "Introduction to antenna and near-field simulation in CST microwave studio software," *IEEE Communication Society, Portugal Chapter*, 2010.
26. Clemens, M. and T. Weiland, "Discrete electromagnetism with the finite integration technique — Abstract," *Journal of Electromagnetic Waves and Applications*, Vol. 15, No. 1, 79–80, 2001.
27. "C. S. T. Studio Suite," in ed: <https://www.cst.com>, 2016.
28. Paul, L. C., M. S. Hosain, S. Sarker, M. H. Prio, M. Morshed, and A. K. Sarkar, "The effect of changing substrate material and thickness on the performance of inset feed microstrip patch antenna," *American Journal of Networks and Communications*, Vol. 4, No. 3, 54–58, 2015.